Lester, D., Lazarovici, P., Pelhate, M., & Zlotkin, E. (1982) *Biochim. Biophys. Acta 701*, 370–387.
Loret, P., Mansuelle, P., Rochat, H., & Granier, C. (1990) *Biochemistry 29*, 1492–1501.
Lowry, O. H., Rosebrough, N. S., Fair, A. L., & Randall, R. J. (1951) *J. Biol. Chem. 193*, 265–275.
Narahashi, T. (1986) in *Neuropharmacology and Pesticide Action.* (Ford, M. G., Lunt, G. G., Reay, R. L., & Usherwood, P. N. R., Eds.) pp 36–70, Ellis Horwood, Chichester, England.
Possani, L. D. (1984) in *Handbook of Natural Toxins* (Tu, T. T., Ed.) Vol. 2, pp 659–678, Marcel Dekker, New York.
Possani, L. D., Martin, B. M., Mochca-Morales, J., & Svendsen, I. (1981) *Carlsberg Res. Commun. 46*, 195–205.
Possani, L. D., Martin, B. M., Svendsen, I., Rode, G. S., & Erickson, B. W. (1985) *Biochem. J. 229*, 739–750.
Reed, L., & Muench, H. (1938) *Am. J. Hyg. 27*, 493–497.
Righetti, P. G., & Chillemi, F. (1978) *J. Chromatogr. 157*, 243–251.
Rochat, H., Rochat, C., Sampieri, F., Miranda, F., & Lissitzky, S. (1972) *Eur. J. Biochem. 28*, 381–388.
Salgado, V. L., Irving, S. N., & Miller, T. A. (1983) *Pestic. Biochem. Physiol. 20*, 100–114.
Sampieri, F., & Habersetzer-Rochat, C. (1978) *Biochim. Biophys. Acta 535*, 100–109.
Swank, R. T., & Munkres, K. D. (1971) Anal. *Biochem. 39*, 463–477.
Walther, D., Zlotkin, E., & Rathmayer, E. (1976) *J. Insect Physiol. 22*, 1187–1194.
Zlotkin (1986) in *Neuroparmacology and Pesticide Action* (Ford, M. G., Lunt, G. G., Raey, R. C., & Usherwood, P. N. R. Eds.) pp 352–383, Ellis Horwood, Chichester, England.
Zlotkin, E., & Gordon, D. (1985) in *Neurochemical Techniques in Insect Research* (Breer, H., & Miller, T. A., Eds.) pp 243–245, Springer, Berlin.
Zlotkin, E., Fraenkel, G., Miranda, F., & Lissitzky, S. (1971a) *Toxicon 9*, 1–8.
Zlotkin, E., Rochat, H., Kopeyan, C., Miranda, F., & Lissitzky, S. (1971b) *Biochimie 53*, 1073–1078.
Zlotkin, E., Kadouri, D., Gordon, P., Pelhate, M., Martin, M. F., & Rochat, H. (1985) *Arch. Biochem. Biophys. 240*, 877–887.
Zlotkin, E., Fishman, L., & Gordon, D. (1988) in *NEUROTOX'88: Molecular Basis of Drug and Pesticide Action.* (Lunt, G. G., Ed.) pp 35–47, Elsevier, Amsterdam.

Fluorescence Study of the Topology of Messenger RNA Bound to the 30S Ribosomal Subunit of *Escherichia coli*†

John Czworkowski, O. W. Odom, and Boyd Hardesty*

Clayton Foundation Biochemical Institute, Department of Chemistry and Biochemistry, The University of Texas at Austin, Austin, Texas 78712

Received December 5, 1990; Revised Manuscript Received February 21, 1991

ABSTRACT: Short RNAs (25–36 nucleotides in length) with sequences of the translational initiation region of bacteriophage R17 protein A mRNA were produced by chemical and in vitro transcription techniques and labeled at their 5′ or 3′ ends with fluorescent probes. The interaction of these labeled RNAs with the 30S subunit of *Escherichia coli* was studied by using fluorescence spectroscopic techniques. All the RNAs bound tightly to 30S subunits ($K_d \leq 200$ nM). Resonance energy transfer experiments demonstrated the proximity of the ends of the RNAs to each other and to two fluorescently labeled sites on the 30S subunit: the 3′ end of 16S rRNA and the cysteine residue of ribosomal protein S21. By using the distances calculated from energy transfer between the 3′ end of 16S rRNA and the ends of RNAs of varying lengths, a topological map of this region of mRNA on the 30S subunit was constructed.

The accumulation of structural information about the ribosome has provided a foundation for inquiries concerning its interaction with the other macromolecules required for protein synthesis. This paper addresses the interaction of mRNA with the 30S subunit. Specifically, fluorescence spectroscopy has been used to study the interaction of short model mRNAs with the subunit and to develop a map of the topology of the mRNA on the 30S subunit by using resonance energy transfer. The model mRNAs possess sequences of the translational initiation region of the A protein of RNA bacteriophage R17 (Steitz, 1969) and are of lengths comparable to the regions of mRNA protected from ribonuclease when bound to the ribosome (Kang & Cantor, 1985; Steitz, 1980).

The site on the ribosome most often implicated by electron microscopy in mRNA binding has been the platform/cleft structure of the 30S subunit, both by direct localization of bound mRNA (Evstafieva et al., 1983) and by localization of important interaction sites for the mRNA such as the 3′ end of the 16S rRNA (Lührmann et al., 1981; Olson & Glitz, 1979; Shatsky et al., 1979), the anti-Shine–Dalgarno region of the 16S rRNA (Olson et al., 1988) and the codon–anticodon interaction site (Gornicki et al., 1984; Oakes et al., 1986). [For a review of ribosome morphology, see Wittmann (1986) and Stöffler and Stöffler-Meilicke (1986).] Evstafieva et al. (1983) have proposed a loop or "U-turn" in the mRNA on the ribosome on the basis of their immunoelectron microscopy studies

†This work was supported by a grant, DMB-87-18579, from the National Science Foundation to B.H.
*Author to whom correspondence should be addressed.

0006-2960/91/0430-4821$02.50/0

of ribosome-bound poly(U).[1] Both the 5′ and 3′ ends of polymers 40–70 nucleotides in length were found on the outer edge of the platform of the 30S subunit, alone and as part of the 70S ribosome. This simple model remains the archetype for the conformation of ribosome-bound mRNA. The model has been supported by determinations of the distance between the ends of ribosome-bound poly(U) by fluorescence energy transfer techniques (Bakin et al., 1987). Affinity labeling of the ribosome by mRNA analogues, and subsequent mapping by comparison to models of ribosomal quaternary structure, have also been carried out (Stade et al., 1989; Vladimirov et al., 1990).

The short model mRNAs used in the following experiments were produced by chemical and in vitro transcription techniques, and all contain a strong Shine–Dalgarno sequence (Shine & Dalgarno, 1974), incorporated to ensure tight binding to the 30S subunit and to afford a positional anchor for the RNAs. A Shine–Dalgarno sequence has been found upstream of the initiation codon in the ribosome binding site of most mRNAs of *Escherichia coli*. This sequence has been shown to base-pair with a sequence at the 3′ end of the 16S rRNA and thereby to promote binding of the initiation region of the mRNA to the ribosome. [For a review see Gualerzi and Pon (1990).]

This report describes experiments involving short model mRNAs labeled with fluorophores at their 3′ or 5′ ends. The effects of binding to the small subunit on the fluorescence properties of the RNAs were studied, and resonance energy transfer between the RNAs and sites on the platform/cleft of the subunit (namely, the 3′ end of the 16S rRNA and protein S21) was measured. By varying the length of the RNAs while maintaining a core sequence, it was possible to develop a map of the mRNA's topology on the 30S subunit with respect to the 3′ end of the 16S rRNA.

Experimental Procedures

Materials. Fluorescent labeling reagents (AETUF, CITC, CPM, DCCH, DCIA, FM, and FTS) were purchased from Molecular Probes, Inc. (Junction City, OR). Ribonucleotides were obtained from Pharmacia-LKB Biotechnology, Inc. (Piscataway, NJ). T7 RNA polymerase and T4 polynucleotide kinase were purchased from New England Biolabs, Inc. (Beverly, MA). RNase T1 from *Aspergillus oryzae* was purchased from Calbiochem Corp. (San Diego, CA). Calf intestinal alkaline phosphatase was obtained from Boehringer-Mannheim Biochemicals (Indianapolis, IN). $tRNA_f^{Met}$ was purchased from Subriden RNA (Rollingbay, WA). Sephadex G50, Bicine, Tris, methionine, and N^5-formyltetrahydrofolate were purchased from Sigma Chemical Co. (St. Louis, MO). The RNase inhibitor RNasin, Hepes, chloroform, DMF, phenol, and triethylamine were obtained from Fisher Scientific (Pittsburgh, PA); DMF, phenol, and triethylamine were redistilled before use. Purified translational initiation factors were a gift of Dr. N. Brot (Roche Institute of Molecular Biology, Nutley, NJ).

Preparation of Ribosomal Subunits and Components. The preparation of ribosomal subunits and 16S rRNA, the 3′ end labeling of 16S rRNA with FTS and subsequent reconstitution into 30S subunits, and the assay of subunit activity by polyphenylalanine synthesis were carried out as described in Odom et al. (1980). The preparation of FM-labeled ribosomal protein S21 and incorporation of this protein into 30S subunits followed the procedure of Odom et al. (1984), except that FM was substituted for CPM.

The initiator aminoacyl-tRNA, fMet-$tRNA_f$, was prepared by the method of Johnson et al. (1982).

Preparation of Model mRNAs. RNA-29[2] was synthesized at Applied Biosystems, Inc. (Foster City, CA), on an Applied Biosystems DNA synthesizer, using 2′-O-silylated ribonucleotides [adapted from Usman et al. (1987)]. The product of the synthesis was purified by reversed-phase HPLC on a C_{18} column with a gradient of acetonitrile in 0.1 M triethylamine acetate (pH 7.0). Chromatography fractions were analyzed on 8 M urea–15% polyacrylamide gels with a buffer containing 90 mM Tris-H_3BO_3 (pH 8.3) and 2 mM EDTA, and were visualized by staining with Stains-All in a 60:40 formamide–water mixture for 1–2 h. RNA-29 eluted from the column at 22% acetonitrile.

RNA-25,26, RNA-30,31, RNA-35,36A, and RNA-35,36B were produced by in vitro transcription according to the procedure of Milligan et al. (1987). The oligodeoxynucleotides used in the transcription reactions were synthesized on an Applied Biosystems DNA synthesizer with nucleotides obtained from Applied Biosystems, Inc. The products of transcription were extracted three times with a 1:1 phenol–chloroform mixture and then purified by chromatography over Sephadex G50 (equilibrated with 25 mM Hepes-NaOH (pH 7.4) and 0.5 M NaCl), removing nucleotides and short abortive transcripts. The RNAs were analyzed by gel electrophoresis as described above for RNA-29.

Preparation of CPTS. The phenylcoumarin thiosemicarbazide CPTS was prepared by reacting CITC with hydrazine, both at a concentration of 0.10 M in DMF. After reaction for 5 min at room temperature, 1.0 mL of 0.2 M sodium acetate (pH 5.0) was added to 100 μL of reaction mixture, and the solution was extracted with an equal volume of ethyl acetate. The ethyl acetate layer was reextracted once with aqueous 0.2 M sodium acetate (pH 5.0); then the ethyl acetate layer, containing the desired product, was evaporated to dryness. The reaction products were analyzed on silica gel thin-layer chromatography plates, with ethyl acetate as the mobile phase. Nearly quantitative conversion of CITC to CPTS was attained.

Fluorescent Labeling of RNAs. RNAs were labeled at the 3′ end with DCCH and CPTS following the method of Odom et al. (1980). 5′ End labeling of RNA-29 with the amine-bearing fluorescein derivative AETUF followed the procedure of Mishenina et al. (1980).

Labeling of the 5′ end of RNAs with the thiol-reactive probes CPM and DCIA required the following: First, transcribed RNAs were dephosphorylated by calf intestinal al-

[1] Abbreviations: AETUF, 5-[(2-aminoethyl)thioureido]fluorescein; ATPγS, adenosine 5′-*O*-(3-thiotriphosphate); Bicine, *N*,*N*-bis(2-hydroxyethyl)glycine; CITC, 7-(diethylamino)-3-(4′-isothiocyanatophenyl)-4-methylcoumarin; CPM, 7-(diethylamino)-3-(4′-maleimidophenyl)-4-methylcoumarin; CPTS, 7-(diethylamino)-3-(4′-thiosemicarbazidophenyl)-4-methylcoumarin; 5′-DCA-RNA, product of reaction of 5′-thiophosphorylated RNA with DCIA; DCCH, 7-(diethylamino)-coumarin-3-carbohydrazide; DCIA, 7-(diethylamino)-3-[4′-[(iodoacetyl)amino]phenyl]-4-methylcoumarin; DMF, dimethylformamide; DTT, dithiothreitol; EDTA, (ethylenedinitrilo)tetraacetic acid; EGTA, ethylenebis(oxyethylenenitrilo)tetraacetic acid; FM, fluorescein-5-maleimide; FTS, fluorescein-5-thiosemicarbazide; Hepes, 4-(2-hydroxyethyl)-1-piperazineethanesulfonic acid; HPLC, high-performance liquid chromatography; IF, initiation factor; poly(U), poly(uridylic acid); RNase, ribonuclease; Tris, 2-amino-2-(hydroxymethyl)propane-1,3-diol; κ^2, dipole orientation factor.

[2] The numbers used to designate the mRNA analogues are their lengths in number of nucleotides. Transcribed RNAs are approximately 1:1 mixtures of n and $n + 1$ polymers; therefore, they are designated with two numbers. RNA-35,36A and RNA-35,36B are of the same length but differ in sequence.

kaline phosphatase (CIAP). The dephosphorylation reaction included 2–3 nmol of RNA and 20 units of CIAP/nmol of RNA, incubated in 300 μL of 40 mM Tris-HCl (pH 8.1) at 50 °C for 60 min. The phosphatase was inactivated by adding EGTA to a concentration of 50 mM and incubating at 50 °C for 30 min further. The mixture was extracted with a 1:1 phenol–chloroform mixture followed by extraction with pure chloroform. NaCl was added to a final concentration of 0.5 M, and the RNA was precipitated with 3 volumes of ethanol at −20 °C. (Note that RNA-29, having been chemically synthesized, does not bear a 5′ phosphate group and therefore did not require this procedure.)

The dephosphorylated RNA was thiophosphorylated at its 5′ end in a 100-μL reaction mixture containing 5 mM ATPγS, 100 units of T4 polynucleotide kinase, 80 units of RNase inhibitor, 70 mM Tris-HCl (pH 7.6), 10 mM $MgCl_2$, and 5 mM DTT; this mixture was incubated at 37 °C for 3 h. The volume was brought to 200 μL and the concentration of NaCl to 0.5 M; the mixture was extracted with a 1:1 phenol–chloroform mixture followed by pure chloroform, and then the aqueous layer was passed over a Sephadex G50 column equilibrated with 25 mM Hepes-NaOH (pH 7.4), 0.5 M NaCl, and 10 mM 2-mercaptoethanol to remove unreacted ATPγS. Fractions containing RNA (determined by absorbance) were pooled and precipitated with ethanol. The precipitate was desiccated thoroughly to remove all 2-mercaptoethanol.

The thiophosphorylated RNA was dissolved in 80 μL of 50 mM Bicine-KOH (pH 8.4). Then 100 μL of DMF was added, followed by 20 μL of 20 mM DCIA dissolved in DMF. The reaction mixture was shaken at room temperature for 4 h, after which the mixture was brought to 1.0 mL with water, extracted, and ethanol-precipitated as described above.

Binding Conditions; RNase T1 Digests. All complexes were formed in binding solution: 40 mM Tris-HCl (pH 7.6), 10 mM magnesium acetate, 100 mM ammonium acetate, and 5 mM 2-mercaptoethanol. Sample volumes were approximately 0.50 mL, containing 10–25 pmol of fluorescent mRNAs. Mixtures were incubated at 37 °C for 15 min before analysis. Digestion by RNase T1 was carried out by adding 5 units of enzyme in 5 μL to the mixture.

Fluorescence Measurements and Analysis. Fluorescence measurements were made with SLM Model 8000 and SLM-Aminco Model 8000C photon-counting spectrofluorometers (SLM Instruments, Urbana, IL), equipped with excitation and emission polarizers. The temperature of the sample was kept constant at 20 °C during measurements. Anisotropy and fluorescence intensity (measured with polarizers at the "magic angle", 54.7°) were determined at the following wavelengths: excitation at 400 nm and emission at 480 nm for CPM-, CPTS-, and DCA-labeled RNAs; excitation at 440 nm and emission at 480 nm for DCCH-labeled RNAs; and excitation at 490 nm and emission at 520 nm for AETUF-, FM-, and FTS-labeled molecules.

The quantum yields of the labeled mRNAs in complex with the 30S subunit were determined by comparison with fluorescence standards. For the DCA-labeled RNAs, quinine sulfate in 0.05 M H_2SO_4 at 25 °C was used as a standard, with a quantum yield of 0.508 (Velapoldi & Mielenz, 1980); the DCCH-labeled RNAs were compared with sodium fluorescein in 0.1 M NaOH at 25 °C, which has a quantum yield of 0.90 (Demas and Crosby, 1971). Emission spectra were scanned at 1-nm intervals and corrected for wavelength-dependent lamp intensity and monochromator sensitivity. The integrals with respect to wavelength were determined (by using Simpson's rule) and the resulting areas were compared. No measurable (i.e., <1% at λ_{max}) change in absorptivity between coumarin-labeled mRNAs in the bound and free states has been observed.

The fraction of RNA bound was determined from the emission anisotropy of the labeled RNA-29 by using

$$x_b = \frac{r - r_f}{(r_b - r)(Q_b/Q_f) + r - r_f} \quad (1)$$

where x_b is the mole fraction of bound to total RNA, r is the steady-state anisotropy measured under the experimental conditions, r_f and r_b are the anisotropies of the free and bound species, respectively, and Q_f and Q_b are the respective quantum yields of the free and bound species (Lakowicz, 1983).

The efficiency of energy transfer, E, was calculated from the quenching of the fluorescence intensity of the donor coumarin adduct, according to

$$E = 1 - F_{DA}/F_D \quad (2)$$

where F_{DA} is the fluorescence intensity of the donor in the presence of acceptor and F_D is the fluorescence intensity of the donor in the absence of the acceptor.

The values of F_D and F_{DA} used in eq 2 were determined from the measured fluorescence of mRNAs in complex with 30S subunits as follows: (1) The fluorescence of two samples of donor-labeled mRNA in binding solution was determined by subtracting the appropriate references from the measured intensity. Every effort was made to make these two samples identical, but any difference in concentration was compensated for by using the measured fluorescence, which at the high dilutions used is proportional to concentration. To one cuvette unlabeled 30S subunits were added, and to the other, (partially) labeled subunits. (The slight dilutions caused by the addition of concentrated subunits were taken into account.) The fluorescence intensity of the former sample, before addition of subunits, will be designated $F_f(D)$, and that of the latter, $F_f(DA)$. (2) After addition of subunits to the cuvettes, scattering (and acceptor-only fluorescence, in the case of F'_{DA}) references were subtracted from the measured intensity of the complexes of donor-labeled mRNA and unlabeled subunits to give F'_D or from that of donor-labeled mRNA and acceptor-labeled subunits to give F'_{DA}. (3) The mole fraction of free mRNA in each cuvette, x_f, was calculated from the measured fluorescence anisotropy according to eq 1 and the relation $x_f = 1 - x_b$. It was assumed that the fraction of 30S subunits that were labeled (60% or 64%, in different experiments) bound mRNA as well as the unlabeled subunits in the mixture. (4) The ratio of the fluorescence of labeled mRNA bound to unlabeled 30S subunits to that of labeled mRNA free in binding solution was calculated as

$$\frac{F_{D,b}}{F_f(D)} = \frac{F'_D - x_f F_f(D)}{F_f(D) - x_f F_f(D)} \quad (3)$$

This ratio was then used to scale the fluorescence of the unbound mRNA to that of the bound, giving a value for F_D that is the fluorescence of the mRNA if totally bound to subunits:

$$F_D = F'_D - x_f F_f(D) + \frac{F_{D,b}}{F_f(D)}[x_f F_f(D)] \quad (4)$$

(5) Equations analogous to eqs 3 and 4 can be written for F'_{DA} (x_f was determined separately for this sample):

$$\frac{F_{DA,b}}{F_f(DA)} = \frac{F'_{DA} - x_f F_f(DA)}{F_f(DA) - x_f F_f(DA)} \quad (5)$$

$$F''_{DA} = F'_{DA} - x_f F_f(DA) + \frac{F_{DA,b}}{F_f(DA)}[x_f F_f(DA)] \quad (6)$$

(6) Any difference in initial concentration of mRNA between the samples was corrected for by adjusting F''_{DA}:

$$F'''_{DA} = [F_f(D)/F_f(DA)]F''_{DA} \quad (7)$$

(7) Finally, the fluorescence of an equal amount of donor-labeled 30S subunits was found by accounting for x_A, the fraction of subunits in the mixture labeled with acceptor:

$$F_{DA} = F_D - (F_D - F'''_{DA})/x_A \quad (8)$$

The results of energy transfer experiments were found to be reproducible, as expected from the above corrections, when mRNA concentration was varied between 20 and 50 nM and 30S concentration was varied between 200 and 300 nM, since in each case the fraction of mRNA bound was determined.

The calculation of energy transfer between the ends of labeled RNA-29 used the intensities of donor-only and donor–acceptor labeled RNAs. Subtraction of reference solutions yielded F_D directly and F'_{DA}, which required further correction. Differences in donor fluorophore concentration between the two samples were corrected by using the ratio of the fluorescence intensity after digestion with RNase T1 (which abolishes energy transfer in the doubly labeled RNA), in an equation similar to eq 7:

$$F''_{DA} = [F_{T1}(D)/F_{T1}(DA)]F'_{DA} \quad (9)$$

Equation 8 was then utilized to adjust for the degree of labeling of the RNA with acceptor; F_{DA} was thereby obtained.

Analysis of the doubly and donor-only labeled RNA-29 yielded the ratio of fluorescence intensity of the donor fluorophore of the two species in solution: $F_{D,f}/F_{DA,f}$. This factor, along with the value for the enhancement of fluorescence of the donor-only labeled RNA on binding 30S subunits, $F_{D,b}/F_{D,f}$, allowed calculation of the fluorescence of the equivalent sample of bound, donor-only labeled RNA-29 from the fluorescence of the doubly labeled RNA-29, according to

$$F_D = F_{DA,f}(F_{D,f}/F_{DA,f})(F_{D,b}/F_{D,f}) \quad (10)$$

Equations 5 and 6 were applied to F'_{DA} (the measured fluorescence of the donor in the doubly labeled RNA when bound to 30S subunits) to account for the small unbound fraction in the mixture. Equation 8 compensated for the fraction of RNAs labeled with acceptor, resulting in the value for F_{DA}.

The fractional uncertainty of F, Q, and E was found to be ≤5% of the mean. The values of E reported were the average of three experiments. Anisotropy values had an uncertainty of ±0.004.

The energy transfer efficiency is related to R, the distance between the probes, by

$$R = (1/E - 1)^{1/6}R_0 \quad (11)$$

where R_0 is the Förster critical distance (Förster, 1949, 1959), i.e., the distance between probes at which E is half-maximal. R_0 was calculated (by using a BASIC program) from the donor emission and acceptor absorption spectra and the quantum yield of the donor. An index of refraction of 1.4 and a dipole orientation factor κ^2 of $^2/_3$ were assumed. Error limits of R due to the κ^2 assumed were calculated from Haas et al. (1978).

RESULTS

Chemically Synthesized mRNA: RNA-29

The initial investigations of the interaction of synthetic model mRNAs with the ribosome were carried out with a chemically synthesized RNA 29-mer, designated here as RNA-29. The sequence of this RNA is as follows: 5′-U*AG-GA GGU*UU GACCU AUG GCA UUC CUG AU-3′. RNA-29 possesses an initiation codon (underlined) and an upstream sequence identical with that in the RNA coding for the A protein of bacteriophage R17 (Steitz, 1969). One feature of this upstream region is a very strong Shine–Dalgarno sequence (italicized), with the potential to form seven base pairs with the 3′ end of the 16S rRNA of the 30S subunit (Shine & Dalgarno, 1974). The strong Shine–Dalgarno sequence was included in RNA-29 to promote tight and specific binding to the subunit.

Table I: Interaction of Fluorescently Labeled RNA-29 with 30S Subunits: Effects on Fluorescence[a]

label	F_{+30S}/F_f[b]	r_f[c]	r_{+30S}[d]
5′-(P)-AETUF	0.96	0.10	0.19
5′-(P)-CPM	1.20	0.20	0.36
3′-DCCH	1.94	0.26	0.36
3′-CPTS	1.20	0.22	0.34

[a] RNA-29 at a concentration between 20 and 50 nM in binding solution was mixed with a 10-fold excess of 30S subunits and preincubated for 15 min at 37 °C. Excitation and emission wavelengths for AETUF were 490 and 520 nm, respectively; for CPM and CPTS, 400 and 480 nm; for DCCH, 440 and 480 nm. [b] F_{+30S}/F_f is the ratio of fluorescence intensity in the presence of excess 30S subunits to that in the free state. [c] r_f is the fluorescence anisotropy of the labeled RNA in the free (unbound) state. [d] r_{+30S} is the fluorescence anisotropy of the labeled RNA in the presence of excess 30S subunits.

RNA-29 was purified in our laboratory by reversed-phase HPLC as described under Experimental Procedures. Fractions from HPLC were analyzed by gel electrophoresis: the RNA product contained approximately 30% (n − 1)-mer (i.e., 28-mer) contaminant.

Labeling of RNA-29 with Fluorescent Probes. Several techniques have been used to label the ends of RNA-29. Chemical labeling of the 5′ end followed the procedure of Mishenina et al. (1980): after the chemically synthesized RNA had been enzymatically phosphorylated at its 5′ end, the monophosphate group was activated with triphenylphosphine and then reacted in the same mixture with a fluorescent amine such as AETUF. This method typically labels 15% of the phosphorylated RNA. Enzymatic labeling requires the initial 5′ thiophosphorylation of RNA-29 with ATPγS by using polynucleotide kinase. The thiophosphate can then be treated with thiol-reactive fluorophores, such as the maleimides (e.g., CPM); 15%–40% overall labeling of the RNA can be attained. Details of the labeling procedure are given under Experimental Procedures.

3′ Labeling of RNA involves first the oxidation of the vicinal diol of the 3′ ribose by periodate to yield aldehydes. The aldehydes will react with fluorescent hydrazides (e.g., DCCH) or semicarbazides (e.g., CPTS) (Odom et al., 1980). Up to 100% labeling of RNA has been achieved with this technique.

Interaction of Fluorescently Labeled RNA-29 with 30S Subunits. RNA-29 was labeled with four different fluorescent probes (AETUF, CPM, DCCH, and CPTS); the effects on fluorescence of the binding of these RNA species to the 30S subunit were observed. An 8–10-fold molar excess of 30S subunits was added to ensure that most RNA-29 was in complex with 30S. All labeled RNAs showed changes in the properties of their fluorescence emissions consistent with strong interaction with the ribosomes (Table I). As would be expected, in all cases a dramatic increase in the steady-state fluorescence anisotropy, r, was observed. This implies a decrease in the rate of rotational diffusion and therefore a restriction in the motion of the probe, a likely effect of the RNA's binding to the much more massive 30S subunit. [For a full discussion of steady-state anisotropy, see Lakowicz (1983).]

Table II: Fluorescence of 5′-CPM-RNA-29: Formation of an Initiation Complex[a]

added components	x[b]	r[c]	F_{rel}[d]
free RNA-29	1	0.20	1.00
+30S subunits	3	0.33	1.29
+fMet-tRNA$_f$, IF-1, IF-2, IF-3	6, 3, 3, 3	0.32	1.31
50S subunits	6	0.31	1.24

[a] All components were mixed in binding solution and incubated for 15 min at 37 °C before measurements were made. [b] x is the molar ratio of an added component to the mRNA, RNA-29. RNA-29 is present at a concentration of 40 nM. [c] r is the steady-state anisotropy of the emission of 5′-CPM-RNA-29 under the conditions described. [d] F_{rel} is the relative fluorescence intensity of 5′-CPM-RNA-29 under the conditions described.

Table III: T1 RNase Digests of Fluorescent RNA-29[a]

conditions	fluorescence anisotropy 5′-CPM	3′-FTS
free RNA-29	0.19	0.12
+T1 (5 min)	0.073	0.038
free RNA-29	0.20	0.12
+30S subunits	0.35	0.25
+T1 (5 min)	0.24	0.037
+T1 (40 min)	0.11	

[a] Effects of digestion on the anisotropy of 5′-CPM-RNA-29 and 3′-FTS-RNA-29, free in binding solution and in a complex with 30S subunits. Labeled RNA-29 was present at a concentration of 40 nM. Where 30S subunits were present, their concentration was 200 nM. Five units of T1 RNase was added to the mixtures and incubated for the indicated times at 37 °C before measurements were made.

Table IV: Energy Transfer from Fluorescently Labeled RNA-29 to Sites within the 30S Subunit

donor	acceptor	E[a]	R/R_0[b]	R'_{max}[c] (nm)
5′-CPM-RNA-29	(3′-FTS-16S)30S	0.53	0.98	5.4
3′-DCCH-RNA-29	(3′-FTS-16S)30S	0.36	1.10	6.0
3′-CPTS-RNA-29	(3′-FTS-16S)30S	0.32	1.13	6.2
5′-CPM-RNA-29	(FM-S21)30S	0.74	0.84	4.6
3′-DCCH-RNA-29	(FM-S21)30S	0.61	0.93	5.1

[a] E is the efficiency of energy transfer. [b] R/R_0 represents the ratio of true distance between donor and acceptor to the distance (R_0) at which the efficiency of energy transfer is half-maximal. [c] R'_{max} is the maximum probable distance between the donor and acceptor probes, assuming $R_0 \leq 5.5$ nm and $\kappa^2 = {}^2/_3$.

RNA-29 labeled with coumarin derivatives (DPM, DCCH, and CPTS) demonstrated an increase in fluorescence intensity on binding to the subunit. This implies that the somewhat nonpolar coumarin moieties, both at the 5′ and 3′ ends of the mRNA, had moved to an environment less polar than the aqueous solution, suggesting binding of the probe to the 30S subunit, perhaps in a groove or cleft. The more polar probe AETUF exhibited only a slight decrease in relative fluorescence upon binding to the subunit, also consistent with expectations for this adduct. Fluorescein derivatives are relatively less sensitive to changes in the polarity of their environment, but a slight decrease in intensity after binding of fluorescein-labeled species to ribosomes has commonly been observed.

Formation of an Initiation Complex. Before peptide synthesis can begin in vivo, several important biomolecules must come together: mRNA, 30S subunits, initiator tRNA, and the initiation factors IF-1, IF-2, and IF-3, and finally 50S subunits. In order to study the interaction of these other components with the mRNA under consideration here, they were added sequentially to 5′-CPM-RNA-29, and the effects on its fluorescence were noted (Table II). Strong evidence of binding was observed upon addition of the first component, 30S subunits: anisotropy and relative fluorescence intensity increased markedly. Subsequent addition of initiator tRNA (fMet-tRNA$_f$), initiation factors, and 50S subunits caused little perturbation, if any.

Ribonuclease Digests of RNA-29: Protection by the 30S Subunit. In order to probe further the nature of the interaction between RNA-29 and the 30S subunit, RNA-29 was subjected to digestion by the ribonuclease T1 from *A. oryzae*. RNase T1 cleaves specifically on the 3′ side of G residues: Gp↓N. The data in Table III show effects of such digests by following the fluorescence anisotropy of the label on the RNA. It can be seen in the upper panel that a short (5-min) incubation at 37 °C with T1 RNase caused a sharp drop in the anisotropy of both the 5′ and the 3′ labels, a result of the much faster rotational diffusion of the short oligonucleotides resulting from the digestion. A much different scenario arose when the RNA was bound to the 30S subunit before T1 RNase was added; these data are presented in the lower panel of Table III. The 3′ label in this case, as in the free RNA, seemed to be quickly cleaved: its anisotropy dropped sharply to the level observed with the free RNA. The anisotropy of the 5′ label, however, remained well above that observed when the free 5′-CPM-RNA-29 was digested, even after incubation for 40 min with the RNase. This is likely a result of greater protection of the 5′ region of the mRNA than of the 3′ end and a strong indication that the probes were in different locations on the subunit. The 5′ probe would demonstrate resistance to being freed from the 30S subunit by RNase digestion if the Shine–Dalgarno base pairs are maintained between RNA-29 and the 16S rRNA in this complex, since double-stranded RNA is much less labile to the enzyme than is single-stranded RNA.

Energy Transfer Studies. With the strong binding between fluorescent RNA-29 and 30S subunits established, it was possible to proceed to studies of resonance energy transfer between the RNA and labeled sites within the ribosome. 30S subunits specifically labeled at sites in the platform/cleft region were used. These were (3′-FTS-16S)30S, 30S subunits labeled at the 3′ end of the 16S rRNA with FTS (Odom et al., 1980), and (FM-S21)30S, 30S subunits labeled site-specifically on the cysteine thiol of ribosomal protein S21 (Odom et al., 1984). Because the anti-Shine–Dalgarno sequence of the 16S rRNA had been localized to the platform region of the 30S subunit (as might be expected due to its proximity to the 3′ end of 16S rRNA), and because the model mRNA RNA-29 contains a strong Shine–Dalgarno sequence, it was thought that the platform region of the small subunit would be a useful positional marker for distance determinations under circumstances where the Shine–Dalgarno interaction was occurring. In addition to energy transfer measurements between RNA-29 and the labeled sites on the 30S subunit, energy transfer between the ends of RNA-29, free in solution and bound to 30S subunits, was also determined.

Data from resonance energy transfer experiments between RNA-29 and labeled 30S subunits are summarized in Table IV. Fluorescein-labeled 30S subunits were present in severalfold molar excess to ensure a high degree of binding of the mRNA in solution. It is obvious that a considerable efficiency of energy transfer (E) was observed between all donor–acceptor pairs tested. Although R_0 was not determined for all the pairs, it has been our experience in this laboratory that energy transfer between coumarin and fluorescein in biomolecules usually involves an R_0 less than 5.5 nm. The rightmost

Table V: Internal Free Energy Transfer within Doubly Labeled RNA-29 (5′-CPM,3′-FTS-RNA-29)

conditions	E	R/R_0	R'_{max}
free	≥0.97	≤0.56	≤3.1
in 30S complex	0.53	0.98	5.4

column of Table IV lists the probable maximum distance between donor and acceptor, assuming $R_0 \leq 5.5$ nm and the orientation factor $\kappa^2 = {}^2/_3$. The following characteristics of the data obtained are noteworthy: (1) Energy transfer between the 5′ end of RNA-29 and the 3′ end of 16S rRNA is quite high, as might be anticipated if the Shine–Dalgarno base-pairing were occurring. Interestingly, however, there is also pronounced energy transfer between the 3′ end of the model mRNA and the 3′ end of 16S rRNA. Considering the fact that RNA-29 would be up to 19 nm in length if outstretched (Yathindra & Sundaralingam, 1975), a folding or looping of the message on the 30S seems likely. (2) Efficiency of energy transfer from the ends of RNA-29 to ribosomal protein S21 is even greater than that to the 3′ end of 16S rRNA, and the distance from the ends of the RNA to (the thiol moiety of) this protein is probably smaller. This finding also supports the folding/looping hypothesis for the mRNA.

The results of internal energy transfer experiments with doubly labeled RNA-29 are shown in Table V. RNA-29 was labeled at its 5′ end with CPM and at its 3′ end with FTS, and the efficiency of energy transfer was determined from the quenching of the fluorescence of the donor, CPM, explained in detail under Experimental Procedures. Important observations are the following: (1) The distance between the ends of doubly labeled RNA-29 free in solution is probably quite small; the upper limit of 3.1 nm is less than the distance (viz., 3.5 nm) between the ends of a randomly coiled RNA of the same length with unrestricted rotation about nucleotide "segments" [calculated from Tanford (1961)]. In fact, greater distance between the ends of an RNA random coil would be expected due to steric hindrances and charge repulsions from the phosphodiester backbone. It is possible that the RNA assumes a more compact structure in solution than is widely conceived for a short RNA molecule with no extensive internal base pairing. A large close loop, with base pairing between nucleotides 2–5 and 23–26 (4 base pairs), and perhaps G-U base pairs between 1 and 27 and between 6 and 22, might be stable enough to account for the high degree of energy transfer, even if the RNA maintains this structure only transitorily. (This base-pairing and the complete Shine–Dalgarno interaction would be mutually exclusive, however.) (2) The efficiency of energy transfer between the ends of RNA-29 bound to 30S subunits is high, and the distance between the probes is near R_0. Taken with the RNase data described above and in Table III, this is further evidence that the ends of RNA-29 are close but in distinctly different locations.

In Vitro Transcribed mRNAs: RNA-25,26, RNA-30,31, RNA-35,36A, and RNA-35,36B

It was found in experiments described above that the 5′ and 3′ ends of a 29-base-long RNA, mimicking an mRNA translation initiation region, were located 5–6 nm from sites in the platform/cleft region of the 30S ribosomal subunit. The investigations now to be described involve analogous experiments with a set of similar RNAs produced by in vitro transcription and varying in length. The core sequence of these RNAs is identical, however, and nearly identical with that of RNA-29. The four sequences studied are shown in Table VI. Note that each polyribonucleotide possesses a strong Shine–Dalgarno sequence (italicized) and an initiation codon (underlined). Due to properties of the transcription system used, each RNA is a mixture (approximately 1:1) of polymers of length n and $n + 1$; T7 RNA polymerase can add an additional random nucleotide after the last template-directed nucleotide.

Table VI: In Vitro Transcribed mRNAs

designation	sequence (5′ → 3′)
25,26	GG*AGGAGGU*UUGACCUAUGGCUUUC
30,31	GG*AGGAGGU*UUGACCUAUGGCUUUCCUGAU
35,36A	GGUCCUU*AGGAGGU*UUGACCUAUGGCUUUCCUGAU
35,36B	GG*AGGAGGU*UUGACCUAUGGCUUUCCUGAUCGACU

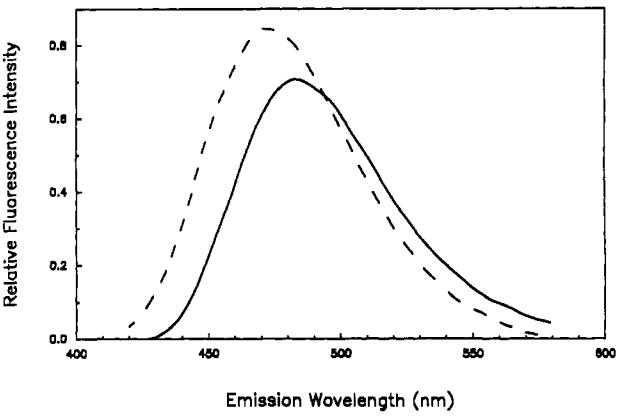

FIGURE 1: Fluorescence emission spectra of 5′-DCA-RNA-25,26 free in binding solution at a concentration of 30 nM (solid line) and in the presence of a 7-fold molar excess of 30S subunits (dashed line).

Synthesis of RNAs. All RNAs in this section were produced by in vitro transcription from oligodeoxynucleotides as described by Milligan et al. (1987). Transcription by T7 RNA polymerase begins at a double-stranded promoter and copies a single-stranded DNA template. After phenol–chloroform extraction and ethanol precipitation, electrophoresis on 8 M urea–15% polyacrylamide gels revealed that about 80% of the RNA product is full-length [n- or $(n + 1)$-mer] transcript. This mixture was further purified of free nucleotides and short abortive transcripts by gel permeation chromatography using Sephadex G50. Gel electrophoretic analysis showed a final product greater than 95% full-length RNA.

Binding of RNAs to 30S Subunits. All the labeled RNAs manifest pronounced differences in the parameters of their fluorescence upon binding to 30S subunits. Spectra of the RNAs bound to subunits invariably displayed an increase in overall intensity and a bathochromic shift. Figure 1 shows sample emission spectra of 5′-DCA-RNA-25,26 free in solution and in the presence of a 7-fold excess of 30S subunits. The 5′-DCA-labeled RNAs increase approximately 25% in emissive intensity, and their emission peaks shift about 10 nm, on addition of the subunits.

3′-DCCH-RNAs demonstrate an increase in fluorescence intensity of >80% on addition of excess 30S subunits, exemplified in Figure 2 by 3′-DCCH-RNA-25,26. A blue shift of the emission peak by 2–5 nm is also apparent.

As a prelude to resonance energy transfer experiments, it was found necessary to determine the fluorescence anisotropy of the various labeled RNAs when completely bound to the 30S subunit, as well as the relative quantum yield in the bound state (i.e., Q_b/Q_f). These two parameters would not only shed light on the environment and mobility of the particular probe on the model mRNA but also allow determination of the fraction of that RNA bound to 30S in any mixture, by using eq 1. In order to make these determinations, a fixed quantity of fluorescently labeled RNA was mixed with increasing

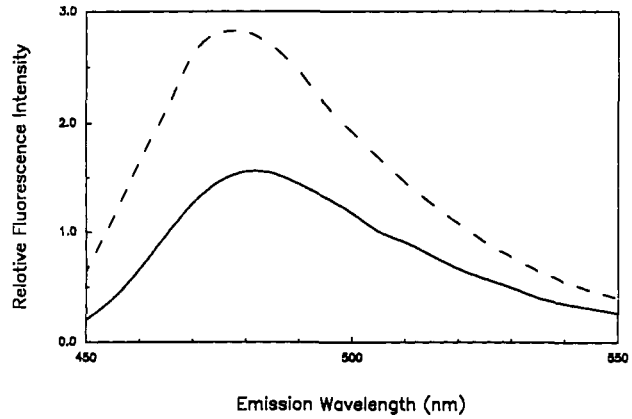

FIGURE 2: Fluorescence emission spectra of 3′-DCCH-RNA-25,26 free in binding solution at a concentration of 40 nM (solid line) and in the presence of a 5-fold molar excess of 30S subunits (dashed line).

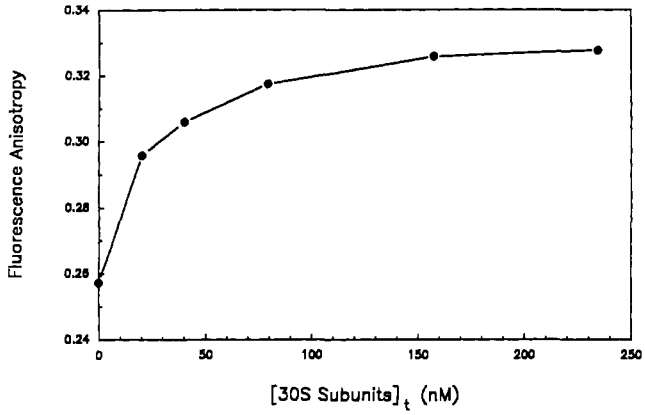

FIGURE 3: Fluorescence anisotropy of 3′-DCCH-RNA-25,26 as a function of the total concentration of 30S subunits in the mixture. 3′-DCCH-RNA-25,26 is present at a concentration of 40 nM.

amounts of 30S subunits. This caused a progressively larger fraction of the RNA present to be bound to the subunits, so that the measured anisotropy and relative quantum yield approached the values of completely bound RNA. An example of the effect of the increase in 30S subunit concentration on the fluorescence anisotropy of 3′-DCCH-RNA-25,26 is shown in Figure 3. First approximations of r_b and Q_b/Q_f were used together with eq 1 to calculate [30S subunits]$_f$ (the concentration of free 30S subunits) and [complex] (the concentration of the 30S subunit·mRNA complex) in each mixture. Next the function ΔQ_{rel} (change in relative quantum yield) vs [30S subunits]$_f$ was fitted by least squares to the binary binding isotherm, with the equations given in Cornish-Bowden (1979); a maximum value for ΔQ_{rel} was found, which is an improved estimate of Q_b/Q_f. The function [complex] vs [30S subunits]$_f$ was likewise fitted by the binding isotherm, and residuals $S^2 = \sum(Y_i - y_i)^2$ were calculated (where Y_i is the observed value of the dependent variable and y_i is the value calculated from the regression line). A new estimate of r_b was made, and the process was iterated, with minimization of the residuals for the binding curve, until the values of r_b and Q_b/Q_f were constant to within 0.2% (Connors, 1987). It was found in this process that approximate values for K_d, the dissociation constant for the binary complex, could be calculated.

The values for r_f, r_b, Q_b/Q_f, and an approximate K_d determined for the DCA- and DCCH-labeled RNAs by the above methods are shown in Table VII. There are several significant features in these data: (1) The fluorescence anisotropy of DCA in 30S-bound 5′-DCA-RNA-35,36A is noticeably lower than in the two other DCA-RNAs studied.

Table VII: Fluorescently Labeled RNAs: Parameters Associated with Binding to Native 30S Subunits

label-RNA	r_f[a]	r_b[b]	Q_b/Q_f[c]	K_d (nM)
5′-DCA-25,26	0.200	0.340	1.28	10
5′-DCA-30,31	0.198	0.332	1.28	<1
5′-DCA-35,36A	0.197	0.300	1.22	30
3′-DCCH-25,26	0.253	0.327	2.00	10
3′-DCCH-29	0.268	0.359	1.94	200
3′-DCCH-30,31	0.263	0.353	2.05	90
3′-DCCH-35,36B	0.271	0.360	2.12	50

[a] r_f is the fluorescence anisotropy of the labeled RNA in the free (unbound) state. [b] r_b is the fluorescence anisotropy of the labeled RNA when bound to 30S subunits. [c] Q_b/Q_f is the ratio of the fluorescence quantum yield in the bound state to that in the free state.

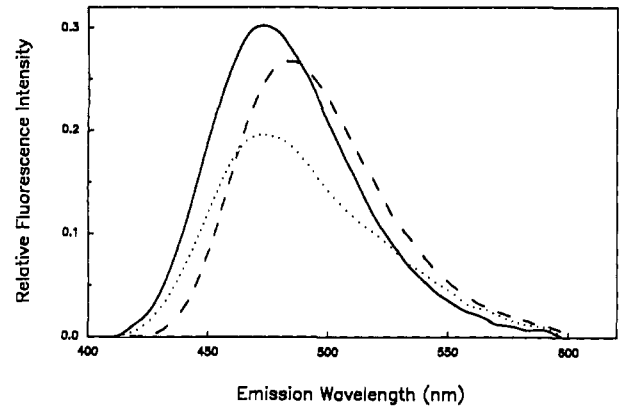

FIGURE 4: Fluorescence emission spectra of 50 nM 5′-DCA-RNA-25,26 alone in binding solution (dashed line), in the presence of 250 nM native 30S subunits (solid line), and in the presence of 250 nM 30S subunits bearing an FTS label on the 3′ end of the 16S rRNA (dotted line).

Both RNA-25,26 and RNA-30,31 have the same 5′ end sequence, so it is likely that their 5′ ends are in the same position relative to the subunit. But RNA-35,36A has an extension of five nucleotides on its 5′ end; the lower r_b indicates a greater freedom of motion of the 5′ end of this RNA and suggests that the message in this region is less restricted—perhaps exiting the binding path or groove for the mRNA on the subunit. (2) The value of r_b for 3′-DCCH-RNA-25,26 is significantly lower than that of the other 3′-DCCH-labeled RNAs. Thus the 3′ end of this RNA has greater flexibility than that of the other RNAs in this group, all of which are extended at their 3′ ends relative to RNA-25,26. The passage of the mRNA through a "window" of exposure to solvent may be implicated. (3) The labeled RNAs have a K_d of binding with the 30S subunit of between 1 and 200 nM.

Energy Transfer Studies between mRNAs and the 3′ End of 16S RNA in the 30S Subunit. The labeled RNAs were next used to study the topology of mRNA on the 30S subunit by distance mapping. An example of spectral data of such an experiment is shown in Figure 4. The fluorescence spectrum of the DCA-RNA in the presence of either native or labeled 30S subunits displays the bathochromic shift indicative of complex formation. However, the fluorescence intensity of the DCA-RNA in the presence of labeled 30S is highly quenched relative to the intensity of the DCA-RNA in the presence of native 30S subunits, even though only 60% of the subunits are labeled with acceptor in these experiments. A slight bulge in the emission spectra of mixtures containing (3′-FTS-16S)30S may be noticed near 520 nm (the emission peak of fluorescein), even though a reference containing only (3′-FTS-16S)30S was subtracted from these spectra. Such a phenomenon would be expected if energy transfer were

Table VIII: Energy Transfer between End-Labeled RNAs and the 3′ End of 16S rRNA in Intact 30S Subunits[a]

label-RNA	$Q_{0,b}$[b]	E	R_0 (nm)	R' (nm)	limits[c] (nm)
5′-DCA-25,26	0.50	0.58	4.8	4.6	3.8–5.5
5′-DCA-30,31	0.50	0.71	4.8	4.2	3.4–4.9
5′-DCA-35,36A	0.48	0.32	4.8	5.5	4.5–6.6
3′-DCCH-25,26	0.15	0.34	4.2	4.7	3.9–5.6
3′-DCCH-29	0.20	0.36	4.4	4.8	4.5–5.8
3′-DCCH-30,31	0.15	0.24	4.2	5.0	4.2–6.0
3′-DCCH-35,36B	0.20	0.26	4.4	5.3	4.4–6.3

[a] The RNA end labels are coumarin fluorophores, acting as donors. The 3′ end of 16S rRNA is labeled with FTS, the energy acceptor. [b] $Q_{0,b}$ is the fluorescence quantum yield of the label on the RNA when bound to the 30S subunit. [c] These are the probable error limits of the distance determined from Haas et al. (1978).

occurring: the fluorescence at 520 nm is due to the enhancement of FTS fluorescence by energy transferred nonradiatively from the coumarin donor.

The results of energy transfer calculations, with the corresponding distance determinations between the ends of the model mRNAs and the 3′ end of 16S rRNA in 30S subunits, are given in Table VIII. For comparison, the values determined for 3′-DCCH-RNA-29 are included in this table. The range of R' between either end of any of the RNAs and the 3′ end of the 16S rRNA falls between 4.1 and 5.5 nm. Distances between (3′-FTS-16S)30S and either 5′-DCA-RNA-25,26 or 5′-DCA-RNA-30,31 are indistinguishable considering the limits of uncertainty expressed in the last column of Table VIII, as might be expected since these two RNAs have identical 5′ sequences relative to the Shine–Dalgarno region. It is conceivable that the difference in length alone between the RNAs is sufficient to cause the difference in the efficiency of energy transfer, E, between the 5′ ends of these RNAs and the acceptor within (3′-FTS-16S)30S; this might be due to a change in the relative orientations of the fluorescent moieties. The probable distance between the 5′ end of 5′-DCA-RNA-35,36A and the 3′ end of the 16S rRNA is considerably greater (by 0.9–1.4 nm) than that for the other two 5′ end labeled RNAs and possibly signifies that the 5′ end upstream of the Shine–Dalgarno sequence is proceeding directly out of the platform/cleft region.

Distances between the 3′ labels and the 3′ end of the 16S rRNA are all quite similar, with only a slight gradual increase (0.6 nm total) in the probable distance as the mRNAs increase at the 3′ end by up to 10 nucleotides. This is clear evidence of the looping, folding, or highly compact structure of the mRNA in this region. (The possibility that the 3′ probes bind to the same hydrophobic site on the subunit cannot yet be excluded.)

Discussion

Fluorescence spectroscopic analyses of the labeled model mRNAs have demonstrated the existence of a tight binary complex with the 30S subunit. The strong binding of short mRNAs containing a Shine–Dalgarno sequence to the 30S subunit, unassisted by initiation factors, has already been described (Calogero et al., 1988; Laughrea & Tam, 1989). In fact, Calogero et al. (1988) have reported a binding constant for their mRNA·30S complex ($K_a = 2 \times 10^7$ M^{-1}) within the distribution of binding constants reported here (Table VII). (That the probes themselves alter the binding of the mRNAs is certainly possible; the extent to which this might occur has not been determined.)

An immediately interesting result of resonance energy transfer experiments between the ends of the mRNAs and the

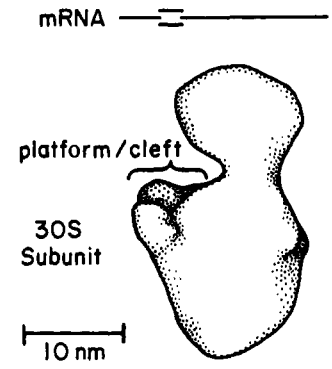

FIGURE 5: Scale drawing of hypothetical mRNA (40-mer) and the 30S subunit [from Verschoor et al. (1984)].

3′ end of 16S rRNA or ribosomal protein S21 was the pronounced transfer efficiency in all cases. The most probable distances, R', were all within 20% of the values of R_0. Calculated distance values between mRNAs and the 3′ end of 16S rRNA in 30S subunits support the "U-turn" hypothesis (Evstafieva et al., 1983), in that the 3′ and 5′ ends of all the RNAs studied were within 6.6 nm of the 3′ end of the 16S rRNA, localized previously to the outer edge of the platform of the 30S subunit (Shatsky et al., 1979; Lührmann et al., 1981). Therefore, one can conclude that the mRNA does not span the 30S in a "straight line". Energy transfer experiments carried out by Bakin et al. (1987) on ribosome-bound poly(U) of lengths 18 and 29 nucleotides found end-to-end distances between 4.4 and 5.4 nm, consistent with the results obtained for natural message sequences in this study and implying a similarity in the topology of the mRNA in the initiation and elongation stages of translation.

A composite of the determined distances has been represented with the use of a hypothetical mRNA of length 40 nucleotides, spanning the sequence from the 5′ end of RNA-35,36A to the 3′ end of RNA-35,36B. This requires the assumption that all the RNAs studied were positioned uniformly by their Shine-Dalgarno sequences in a groove or trough. The hypothetical 40-mer is depicted in Figure 5 as an outstretched RNA above a scale drawing of the 30S subunit [from Verschoor et al. (1984)]. The double line on the RNA is the Shine–Dalgarno region, drawn at the length of double-helical RNA, 0.28 nm/residue (Arnott et al., 1975); the rest of the RNA was drawn as a single strand at 0.68 nm/residue (Yathindra & Sundaralingam, 1975). Clearly, with a length of 24 nm, this 40-mer could traverse the width of the small subunit. A two-dimensional topological map of this 40-mer with respect to the 3′ end of the 16S rRNA is shown in Figure 6. The length of the RNA is to the scale described above. Dashed lines represent the distances determined in energy transfer experiments, used as tethers between labeled positions. Thus the arrangement is flexible within the bounds of the RNA length and the distance tethers.

The map arranges the 40-mer rather compactly around the 3′ end of the 16S rRNA. The 5′ end is moving away from the 16S, and anisotropy data suggest it may be exiting the subunit. The segment containing the initiation codon is shown stretched out as a loop away from the 3′ end of the 16S rRNA; at its maximum probable distance of approximately 7 nm, it would be well in range of the cleft of the 30S subunit, the site at which the codon–anticodon interaction had previously been localized (Gornicki et al., 1984; Oakes et al., 1986). This mRNA topology would therefore be consistent with models placing the codon–anticodon interaction site deep in the cleft of the small subunit and would preclude this mRNA's wrapping around the neck of the subunit. [Nothing can be said

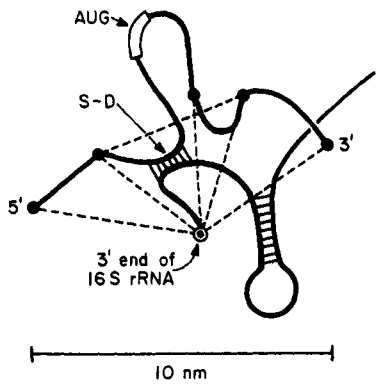

FIGURE 6: Two-dimensional topological map of the hypothetical 40-mer mRNA with respect to the 3' end of 16S rRNA on the 30S subunit. Dashed lines represent distance tethers derived from energy transfer data. S-D: Shine–Dalgarno interaction.

of the topology of stretches of message downstream (3') of the hypothetical mRNA, of course.] Thus it would seem that the hypothetical RNA 40-mer is bound entirely in the platform/cleft of the subunit.

The interaction between mRNA sequences downstream from the initiation codon and the 3' end region of the 16S rRNA during the elongation stage of peptide synthesis has been reported (Weiss et al., 1988; Sprengart et al., 1990) and suggests that downstream regions of mRNA continue to pass close to the 3' end of 16S rRNA after the initiation of translation. This circumstance would arise if the mRNA continued during elongation to travel along the path described by the topology presented here.

Localization of the anti-Shine–Dalgarno sequence of 16S rRNA in the small subunit by electron microscopy of antibody–oligodeoxynucleotide complexes was carried out by Olson et al. (1988). They concluded that mRNA in the Shine–Dalgarno region proceeds 5' → 3' from the tip of the platform of the 30S subunit "downward" toward the base of the platform, near the neck of the subunit.

The cross-linking studies of Stade et al. (1988) found extreme 3' regions of the 16S rRNA, as well as a large number of ribosomal proteins, cross-linked to their mRNA analogues, where the photoreactive group was present between the Shine-Dalgarno sequence and the initiation codon. In the absence of tRNA, the ribosomal protein cross-linked to the greatest extent was S21, but in the presence of cognate tRNA, a much larger amount of protein S7 (localized by immunoelectron microscopy to the head of the 30S subunit, facing the platform) was cross-linked to the mRNA. This led the investigators to propose a switch in the conformation of the mRNA on binding of the cognate tRNA. They further stated that their results support the suggestion of Olson et al. (1988) that the mRNA leaves the subunit in a "northerly" direction out of the cleft—even though no differential cross-linking dependent on the location of the photoreactive group within the mRNA was reported.

The mRNA analogue–ribosome cross-linking experiments of Vladimirov et al. (1990) show cross-linking of mRNA to many ribosomal proteins. The mRNA analogues used were reactive forms of U_n or $AUGU_n$ (n = 3–6). Data were interpreted to indicate binding of mRNA in the region of the platform/cleft of 30S as well as [in the case of 5'-labeled oligo(U)] in the region of the small lobe and neck of the 30S distal from the platform.

In addition to its widespread agreement with experimental evidence, the model presented here is also in agreement with the theoretical proposal of a "kink" in the intercodon juncture of the mRNA, a result of analysis of the steric requirements of adjacent tRNAs involved in peptide bond formation (Rich, 1974; Sundaralingam et al., 1975; Spirin & Lim, 1986). The model in Figure 6 places the initiation codon and second codon at the end of a narrow loop. Alternatively, this region of the mRNA may exist in a compacted conformation. Either structure would be conducive to the kinking of the message near the initiation codon.

ACKNOWLEDGMENTS

We are grateful to Dr. K. Browning for the preparation of oligodeoxynucleotides and for her advice in the production of RNAs, to R. Keegan for artwork and photography, and to Dr. G. Kramer for review of the manuscript.

Registry No. RNA-29, 133227-75-5; RNA-25,26, 133227-74-4; RNA-30,31, 133227-76-6; RNA-35,36A, 133227-77-7; RNA-35,36B, 133227-78-8.

REFERENCES

Arnott, S., Chandrasekaran, R., & Selsing, E. (1975) in *Structure and Conformation of Nucleic Acids and Protein–Nucleic Acid Interactions* (Sundaralingam, M., & Rao, S. T., Eds.) pp 577–596, University Park Press, Baltimore, MD.

Bakin, A. V., Evstaf'eva, A. G., Borisova, O. F., Shatskii, I. N., & Bogdanov, A. A. (1987) *Dokl. Akad. Nauk SSSR 294*, 988–991.

Calogero, R. A., Pon, C. L., Canonaco, M. A., & Gualerzi, C. O. (1988) *Proc. Natl. Acad. Sci. U.S.A. 85*, 6427–6431.

Connors, K. A. (1987) *Binding Constants: The Measurement of Molecular Complex Stability*, John Wiley and Sons, New York.

Cornish-Bowden, A. (1979) *Fundamentals of Enzyme Kinetics*, Butterworths and Co., Ltd., London.

Dawson, W. R., & Windsor, M. H. (1968) *J. Phys. Chem. 72*, 3251–3260.

Demas, J. N., & Crosby, G. A. (1971) *J. Phys. Chem. 75*, 991–1024.

Evstafieva, A. G., Shatsky, I. N., Bogdanov, A. A., Semenkov, Y. P., & Vasiliev, V. D. (1983) *EMBO J. 2*, 799–804.

Förster, T. (1949) *Z. Naturforsch. A 4*, 321–327.

Förster, T. (1959) *Discuss. Faraday Soc. 27*, 7–17.

Gornicki, P., Nurse, K., Hellmann, W., Boublik, M., & Ofengand, J. (1984) *J. Biol. Chem. 259*, 10493–10498.

Gualerzi, C. O., & Pon, C. L. (1990) *Biochemistry 29*, 5881–5889.

Haas, E., Katchalski-Katzir, E., & Steinberg, I. Z. (1978) *Biochemistry 17*, 5064–5070.

Johnson, A. E., Adkins, H. J., Matthews, E. A., & Cantor, C. R. (1982) *J. Mol. Biol. 156*, 113–140.

Kang, C., & Cantor, C. R. (1985) *J. Mol. Biol. 181*, 241–251.

Lakowicz, J. R. (1983) *Principles of Fluorescence Spectroscopy*, Plenum Press, New York.

Laughrea, M., & Tam, J. (1989) *Biochem. Cell Biol. 67*, 812–817.

Lührmann, R., Stöffler-Meilicke, M., & Stöffler, G. (1981) *Mol. Gen. Genet. 182*, 369–376.

Milligan, J. F., Groebe, D. R., Witherell, G. W., & Uhlenbeck, O. C. (1987) *Nucleic Acids Res. 15*, 8783–8798.

Mishenina, G. F., Samukhov, V. V., & Shubina, T. N. (1980) *Bioorg. Khim. 5* (6), 886–894.

Oakes, M., Clark, M. W., Henderson, E., & Lake, J. A. (1986) *Proc. Natl. Acad. Sci. U.S.A. 83*, 275–279.

Odom, O. W., Robbins, D. J., Lynch, J., Dottavio-Martin, D., Kramer, G., & Hardesty, B. (1980) *Biochemistry 19*, 5947–5954.

Odom, O. W., Deng, H.-Y., Dabbs, E. R., & Hardesty, B. (1984) *Biochemistry 23*, 5069–5076.

Olson, H. M., & Glitz, D. G. (1979) *Proc. Natl. Acad. Sci. U.S.A. 76*, 3769–3773.

Olson, H. M., Lasater, L. S., Cann, P. A., & Glitz, D. G. (1988) *J. Biol. Chem. 263*, 15196–15204.

Rich, A. (1974) in *Ribosomes* (Nomura, M., Tissières, A., & Lengyel, P., Eds.) pp 871–884, Cold Spring Harbor Laboratory, Cold Spring Harbor, NY.

Shatsky, I. N., Mochalova, L. V., Kojouharova, M. S., Bogdanov, A. A., & Vasiliev, V. D. (1979) *J. Mol. Biol. 133*, 501–515.

Shine, J., & Dalgarno, L. (1974) *Proc. Natl. Acad. Sci. U.S.A. 71*, 1342–1346.

Spirin, A. S., & Lim, V. I. (1986) in *Structure, Function, and Genetics of Ribosomes* (Hardesty, B., & Kramer, G., Eds.) pp 556–572, Springer-Verlag, New York.

Sprengart, M. L., Fatscher, H. P., & Fuchs, E. (1990) *Nucleic Acids Res. 18*, 1719–1723.

Stade, K., Rinke-Appel, J., & Brimacombe, R. (1989) *Nucleic Acids Res. 17*, 9889–9908.

Steitz, J. A. (1969) *Nature 224*, 957–964.

Steitz, J. A. (1980) in *Ribosomes, Structure, Function, and Genetics* (Chambliss, G., et al., Eds.) pp 479–496, University Park Press, Baltimore, MD.

Stöffler, G., & Stöffler-Meilicke, M. (1986) in *Structure, Function, and Genetics of Ribosomes* (Hardesty, B., & Kramer, G., Eds.) pp 28–46, Springer-Verlag, New York.

Sundaralingam, M., Brennan, T., Yathindra, N., & Ichikawa, T. (1975) in *Structure and Conformation of Nucleic Acids and Protein–Nucleic Acid Interactions* (Sundaralingam, M., & Rao, S. T., Eds.) pp 101–116, University Park Press, Baltimore, MD.

Tanford, C. (1961) *Physical Chemistry of Macromolecules*, John Wiley and Sons, New York.

Usman, N., Ogilvie, K. K., Jiang, M.-Y., & Cedergren, R. J. (1987) *J. Am. Chem. Soc. 109*, 7845–7854.

Velapoldi, R. A., & Mielenz, K. D. (1980) *A Fluorescence Standard Reference Material: Quinine Sulfate Dihydrate*, National Bureau of Standards Special Publication 260-64, U.S. Government Printing Office, Washington, DC.

Verschoor, A., Frank, J., Radermacher, M., Wagenknecht, T., & Boublik, M. (1984) *J. Mol. Biol. 178*, 677–698.

Vladimirov, S. N., Babkina, G. T., Venijaminova, A. G., Gimautdinova, O. I., Zenkova, M. A., & Karpova, G. G. (1990) *Biochim. Biophys. Acta 1048*, 245–256.

Weiss, R. B., Dunn, D. M., Dahlberg, A. E., Atkins, J. F., & Gesteland, R. F. (1988) *EMBO J. 7*, 1503–1507.

Wittmann, H. G. (1986) in *Structure, Function, and Genetics of Ribosomes* (Hardesty, B., & Kramer, G., Eds.) pp 1–27, Springer-Verlag, New York.

Yathindra, N., & Sundaralingam, M. (1975) in *Structure and Conformation of Nucleic Acids and Protein–Nucleic Acid Interactions* (Sundaralingam, M., & Rao, S. T., Eds.) pp 649–676, University Park Press, Baltimore, MD.